Digest Journal of Nanomaterials and Biostructures Vol. 11, No. 1, January - March 2016, p. 105 - 114

PREPARATION AND CHARACTERIZATION OF POLYSTYRENE/ORGANOCLAY NANOCOMPOSITES FROM RAW CLAY

L. A. AL JUHAIMAN*, D. A. AL-ENEZI†, W. K. MEKHAMER
Chemistry Department, King Saud University, Riyadh , Saudi Arabia

Polystyrene/clay nanocomposite (PCN) was successfully prepared. Five characterization methods were applied: Particle size distribution analysis (PSD), Fourier Transfer Infrared spectra (FTIR), X-ray diffraction (XRD), Transmission Electronic Microscopy (TEM) and Differential Scanning Calorimetry (DSC). PCN was prepared by modification of Raw Kholais clay first with NaCl then with Cetylpyridinium chloride (CPC) surfactant to obtain the organoclay (OC). After ion exchange with CPC, FTIR confirmed the existence of these intercalated agents in the organic clay samples. PSD showed that the size of the monodispersed particles of Na-clay was about 1335 nm while the OC shows one peak with a narrow size distribution in the histogram of 738nm which indicate that a homogenous polymer/clay nanocomposites will be obtained. The preparation of polystyrene/OC nanocomposites was accomplished by solution blending method at different ratios of OC. They were labelled 1%, 3%, 5% and 10% NC. PCN films were characterized using XRD and TEM. Exfoliated structure was obtained for the low clay loading (1-5 % NC) while intercalated structure was probably the predominated form in the case of 10% NC. DSC showed that T_g at low clay content (1-5 wt %) decreased compared to pure polystyrene which reflected the plasticization effect of the organic modifier.

(Received December 1, 2015; Accepted January 22, 2016)

Keywords: Raw clay; Polystyrene; Fourier Transfer Infrared spectra (FTIR); X-ray diffraction (XRD); Transmission electronic microscopy (TEM); Nanocomposite.

1. Introduction

In recent years, Polymer–Clay Nanocomposite (PCN) had attracted intrest in engineering and science [1, 2]. PCN is a new class of materials obtained by the dispersion of a few weight percent of clay in the nanometer scale within the polymer matrix which lead to unique physical, chemical and physicochemical properties [3-8]. Usually, PCN is prepared by three methods: in-situ polymerization, solution blending method and melt intercalation. The structures of PCN are classified into intercalated, flocculated and exfoliated nanocomposites [9-12]. These PCN structures depend on the strength of the interfacial interactions between the polymer matrices and the clay [7, 13, 14].

Smectite is the most commonly clay used for the preparation of Polymer-Clay nanocomposites because it is environmentally friendly, naturally abundant and has a huge cationic exchange capacity. Smectite belongs to the 2:1 phyllosilicates family that has a crystal structure composed of the octahedral sheet of alumina sandwiched between two tetrahedral sheets of silica [7, 8]. Negative charges were generated on the clay surface through isomorphic substitution within the layers. The gap between the layers is called the gallery or d001 spacing that may vary depending on the size of the adsorbed cations. The surface and galleries of clay are hydrophilic in nature, but they may be changed to an organophilic one by ion exchange using a surfactant. Large interlayer spacing occurs when the hydrated cations are ion exchanged with organic cations such as alkyl ammonium cations [7].

*Corresponding author: ljuhiman@ksu.edu.sa;

Modification of clay layers with the cationic surfactant is necessary to render the clay layers more compatible with the polymer chains [2-6, 14-28]. The organoclay with lowered surface energy are more compatible with polymers, and polymer molecules can intercalate within their interlayer space or galleries under well-defined experimental conditions. Polystyrene is an inexpensive resin per unit weight. It is a poor barrier to oxygen and water vapor (this properties is necessary for preparing anticorrosive coating film.

Although there are many reports on the synthesis of PCN [3-6, 9-12, 14-28], most previous studies were using pretreated clay (obtained from the market) in the preparation of polymer clay nanocomposites. To the best of our knowledge, the previous studies utilized different combinations of clay, surfactant, and methods in their preparation. Moreover, the difference in clay composition will produce a different PCN with unique properties. The following characterization methods were employed: PSD, FTIR, XRD TEM, and DSC. Thus, the main goal of the present study is: First to obtain the raw clay (RC) from Kholais region in Saudi Arabia with the help of a certified geologist then to perform all the required modification in our lab. Secondly, RC was treated with NaCl to obtain Na-clay (NaC). The third step was the synthesis of organoclay (OC) by the cationic surfactant, Cetylpyridinium chloride (CPC). Finally Polystyrene/OC nanocomposites (NC) were prepared using solution blending method at a different content of OC.

2. Experimental

2.1. Materials

A raw clay (**RC**) was collected by a certified geologist from the north western part of the country. It was ground in our laboratory using a ball mill. The raw clay was characterized by X-ray diffraction (XRD). Depending on a previous study on Kholais clay by Mekhamer [13], the dominant component is montmorillonite (35.22%) as shown in Fig. 1. The other components are kaolinite (13.33%), mica (22.80%), quartz (8.57%), feldapars (6.66%), and ilmenite (5.71), dolomite (3.81%) and gypsum (3.81%). The chemical composition was found by Mekhamer [13]. The X-ray Florescence (XRF) data is presented in Table 1 [13]. Calculations based on the X-ray florescence (XRF) data of this clay sample to find out the structural formula of the montmorillonite existed in this sample.

$Na_{0.67}\ K_{0.13}Ca_{0.02}Ba_{0.04}\ (Si_{7.47}\ Al_{0.53})\ (Al_{2.59}\ Fe_{0.78}Ti_{0.14}\text{-}Mg_{0.44}\ Cr_{0.04})O_{20}(OH)_4$.

The bold color ions represent the exchangeable ions. The first bracket is for silica tetrahedral but the second for aluminum or ferric octahedral. The surface area was measured by BET in a previous paper by Al-Qunabit and Al Juhaiman as $37 m^2/g$ [14]. The cation exchange capacity (CEC) of the raw clay was determined. Polystyrene (PS) was purchased from Sabic Company, Kingdom Saudi Arabia, (M=259,000 g/mol). Cetylpyridinium chloride (CPC, ($C_{21}H_{38}ClN.\ H_2O$) M =358.01 g/mol) with a purity of 98% was provided by BDH. It was used as a cationic surfactant. Toluene with 99.5% purity was used as a solvent (provided by Avonchem Co.).

Table 1: Chemical composition of raw bentonite used in the present study [13]

SiO_2	Al_2O_3	Fe_2O_3	MgO	CaO	Na_2O	K_2O	TiO_2	Impurities
70.30%	15 %	7.75%	2.30%	1.60%	1.45%	1.20%	0.30%	0.10 wt.%

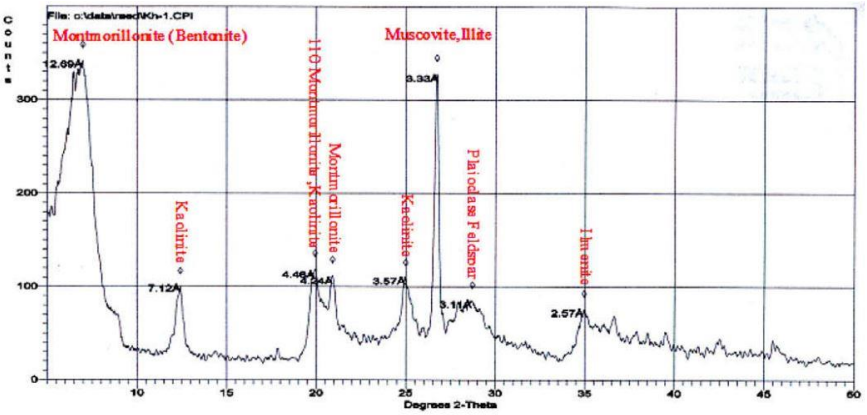

Fig. 1. X-ray diffraction of raw Clay [13]

2.2. Separation and saturation of clay

Fifty grams of raw untreated clay (RC) was dispersed in 500ml of distilled water, shaken for 2 h then left overnight. The supernatant solution was decanted and the process was repeated three times. Then, 300 ml of 0.5 M NaCl solution was added to the clay and the suspension was mixed by shaking for 2 hours then left overnight. This process was repeated three times. In order to remove the excess salt, the Na-saturated clay was washed with distilled water and separated by centrifuging until the $AgNO_3$ test for chloride was negative. The sodium saturated clay (NaC) thus obtained was dried at 120 $^{\circ}$C, and finally crushed in a mortar and stored in a desiccator over $CaCl_2$.

2.3. Preparation of PS/OC nanocomposites

The organoclay (OC) was prepared by a cation-exchange reaction between the sodium cations of NaC and cetylpyridinium chloride cations. The role of the alkyl ammonium cations in the organosilicates is to lower the surface energy of the inorganic clay and improve the wetting characteristics with the polymer [5]. Five grams of NaC was dispersed in 500 ml distilled water, and the dispersion was stirred vigorously overnight. The cation exchange capacity (CEC) of the resulted clay was 85 meq/100 g. The amount corresponding to 2 times the CEC of clay of Cetylpyridinium chloride was dissolved in 100 ml distilled water. The CPC solution was added to the NaC suspension at a rate of 1ml/10min with vigorous stirring and the mixture was stirred for 24 h at room temperature [4]. The resulting organoclay (OC) was separated by centrifugation and washed with distilled water several times until no chloride ions were detected by 0.1M $AgNO_3$ solution. Finally, the OC was dried at 60 ˚C for 24 h in oven.

Polystyrene/OC nanocomposites (PCN) were prepared at different content of OC (0, 1, 3, 5 and 10 wt %). The symbols of PCN prepared in the present study are labelled 1%NC,3%NC,5%NC and 10%NC. In a 50 ml flask, a certain mass of OC was added to 10 ml toluene. This suspension was stirred magnetically overnight at room temperature, then 2 g of PS was added. The mixture was stirred magnetically for 6 hours and in ultrasonic machine for 10 minutes before casted into petri dishes allowing the toluene to evaporate. For film preparation, the solution was casted onto a substrate (e.g. a microscope glass slide). The preparation of the PCN is illustrated in the Scheme 1.

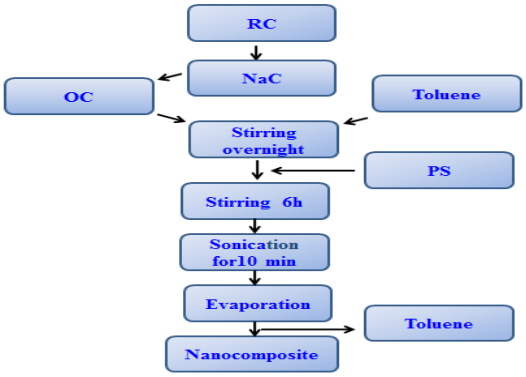

Scheme 1. Preparation of PS/OC nanocomposites

2.4. Characterization method

2.4.1. Fourier transform infrared spectroscopy (FTIR):

FTIR was performed to observe the effect of the clay modification in the range 4000-400 cm^{-1} using FT-IR Spectrometer 1000, Perkin Elmer. Thin films of dimensions 1cm x1cm were used.

2.4.2. Particle size distribution analysis (PSD):

PSD is a measurement designed to determine and report information about the size and range of sizes of a set of particles of a material. The particle size analysis of Na-MMT and O-MMT suspension was determined by using Particle Size Analyzer SA-CP2 model Shimadzu Crop (zetasizer).

2.4.3. X-Ray Diffraction (XRD):

The structure of the nanocomposites was monitored by analytical XPERT-PRO X-Ray Diffractometer (Holland), equipped with Cu anode radiation (λ= 1.540 A^o) source operated at a generator tension of 40 kV and a generator current of 40 mA. The diffraction patterns were collected at diffraction angle 2θ from 3 to 50^o. Thin films of dimensions 1cm x1cm were used.

2.4.4. Transmission electron microscopy (TEM):

TEM images were recorded on a JEOL JSM-6060 LV Transmission Electron Microscope. The samples were embedded in an epoxy resin and cured overnight at room temperature.

2.4.5. Differential scanning calorimeter (DSC):

DSC analysis was performed using a General V4.1.C DuPont 2000. The measurements were carried out in the temperature range of 25-200°C with a heating rate of 10°C/min, followed by cooling at the same rate under nitrogen atmosphere to prevent oxidation. All the analyses were performed on the 2nd run.

3. Results and Discussion

3.1. Fourier Transfer Infrared spectra (FTIR)

The full FTIR spectra of RC, NaC and OC samples are illustrated in Fig. 2. For RC, the bands at 3696 cm-1 and 3625 cm-1, are due to -OH band stretching for Si-OH and Al-OH, respectively. The interlayer water gives a broad band at 3428 cm-1 corresponding to the stretching vibrations for the hydroxyl group, and the absorption band of -OH bending at 1637 cm-1 [15-17]. The strong absorption bands at 1032 cm–1 is ascribed to Si-O stretching vibrations of layered silicates, bands at 528 and 466 cm-1 are related to the Al-O-Si bending and Si-O-Si bending vibrations [15]. The absorption bands for NaC are 3627 cm-1(-OH stretching vibration of (Al-OH), 1033 cm-1(Si-O stretching vibrations). The absorption bands of NaC also found at 3432,

1632 cm-1are characteristic of the stretching and bending vibrations of the interlayer water of layered silicates [16, 17]. The bending-in-plane vibrations of the –OH groups in NaC at 1632cm-1 shifted to 1636 cm-1 in the FTIR of the OC sample. The broad band observed in NaC at 3432 cm-1 corresponds to the stretching vibrations of OH (interlayer water) shifted to 3428 cm-1 in OC, due to the intercalation of surfactant molecules. A pair of strong peaks at 2915 and 2849 cm−1, can be assigned to the asymmetric and symmetric stretching vibrations of the C-H in the alkyl chains of the CPC molecules [15-27]. These sharp peaks shifted to 2929 and 2852 cm−1, indicating the intermolecular attractions between adjacent alkyl chains of CPC in NaC galleries [17, 27].

FTIR spectra of OC, PS, and PS/OC nanocomposite (PCN) at different contents of OC are shown in Fig. 3. Apparently there is not much difference for the FTIR spectrum of PS/OC nanocomposite (Fig. 3.) spectra to PS spectrum. However, an increase could be observed at the peak intensity of the band (1027 cm−1) which can be due to the Si–O absorption [17]. For 10% NC, a broad band was observed at 1031 cm-1 that is attributed to the Si-O stretching vibrations of OC. On increasing the OC content, the band at 2922 cm-1 in PS (aliphatic C-H stretching) shifted slightly to a lower wavenumbers in PS/OC nanocomposites. Also, for pure PS, the vibrational band at 738 cm-1 (C-H bnding) shifted to a higher wavenumber in PS/OMMT nanocomposites; these shifts may be attributed to the dispersion of OC in the PS matrix [15, 16].

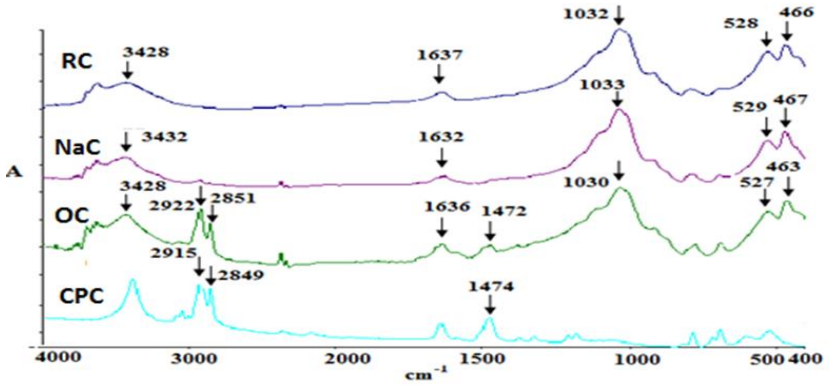

Fig. 2. FTIR spectra of RC, NaC and OC

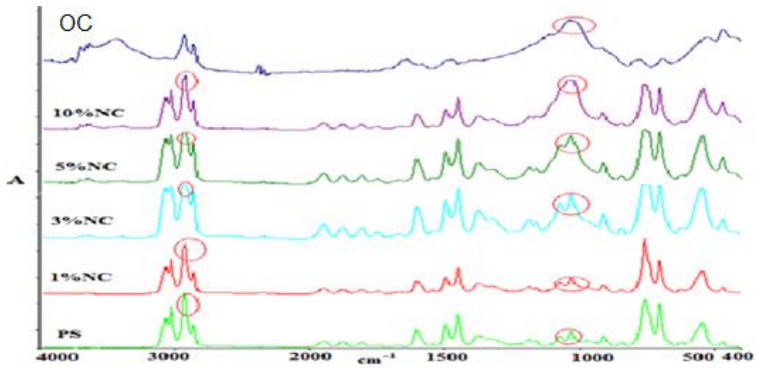

Fig.3. FTIR spectra of OC, PS and PCN

3.2. A particle size distribution analysis (PSD)

PSD is a measurement designed to determine and report information about the size and range of sizes of a set of particles of a material. Fig. 4. shows the size distribution histogram of NaC and OC suspensions. The size of the monodispersed particles of NaC was about 1335 nm (1.3μm) while the OC shows one peak with a narrow size distribution in the histogram, which may be related to one type of size distribution. This result revealed that the particle size of OC to be

highly monodispersed particles of about 738 nm indicating that they have the same size. Decreasing the particle size of OC is one of the features which help to spreading clay particles between the polymer matrixes, so homogenous polymer/clay nanocomposites will be obtained.

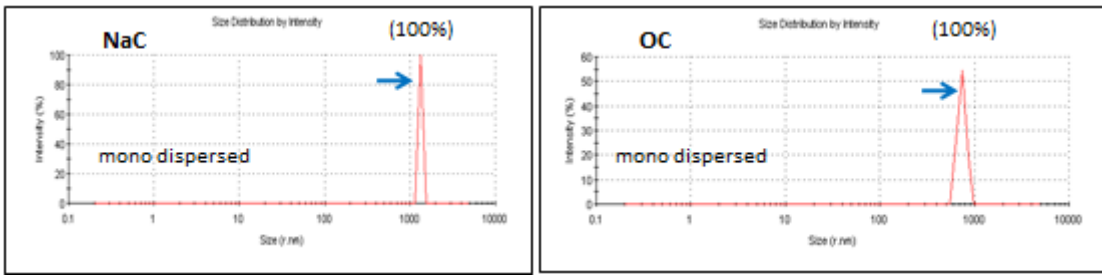

Fig. 4. Particle size distribution of NaC and OC

3.3. X-Ray Diffraction (XRD)

The XRD of RC, NaC, OC, and PS/OC nanocomposites were recorded at 2θ = 3-50° as shown in Fig. 5. The d-spacing's of the nanocomposites were calculated from the angular positions 2Θ of the observed (001) reflection peaks based on the Bragg formula

$$\lambda = 2d\sin\Theta$$

where λ is the wavelength of the X-ray beam (λ= 1.540 A°)) and Θ is the scattering angle. For RC, the inter gallery distance between the clay layers appeared at 2θ=6.46° corresponding to a d_{001} spacing of 13.67 Å while the NaC exhibits a sharp reflection at 2θ =7.07° (d_{001} spacing =12.5 Å). After modification by the surfactant (CPC), an increase in the d100 spacing was observed for OC that appeared at 2θ= 4.1° (21.49 Å) which agrees with many previous studies [18-23]. One of the most important properties of layered silicates is the inter gallery distance (d001) between the clay layers. The large increase in the interlayer distance after the modification confirms the exchange of the interlayer sodium ions by the organic long-chain cations of (CPC). The large increase in d001 spacing implies that the organic modifier is incorporated between clay layers and pushing them into a wider distance [18-20].

A previous study [18] showed that the monolayer is formed when basal spacing is about 13.7Å, the bilayer at 17.7Å, the pseudo trimolecular layer at 21.7Å and paraffin complex with basal spacing greater than 22Å. Depending on the above probable mechanism, the large increase in d-spacing of OC (21.49 Å) indicates that the structural configuration of alkyl chains of CPC ranged between the bilayer and pseudo trimolecular layer. The d-spacing in the present work (21.49 Å) is higher than the d-spacing in a previous work (19.6 Å) using the same Kholais clay but modified by (CTAB) [17]. Cetyltrimethylammonium bromide (CTAB) has the molecular formula of $C_{19}H_{42}NBr$, MW=364·46) whereas Cetylpyridinium chloride has the molecular formula of $C_{21}H_{38}ClN$. H_2O. The increase in d spacing is probably attributed to the increase in the number of carbon atoms. This result is in agreement with other studies which indicated that the increase in d-spacing of OC depends on the structure of surfactant used [5, 16, 21].

As for the XRD patterns of OC one nanocomposite structure is possible, the diffraction peak of the silicate layers shifted towards a smaller angle (2θ < 10o) and seen at a larger d-spacing that indicates an intercalated structure [15-18]. Another possible nanocomposite structure is the exfoliated structure where the diffraction peaks are not visible in the XRD diffractograms either because of too large spacing between the layers or because the nanocomposite does not present ordering. The XRD pattern of pure PS does not produce sharp peaks, only an amorphous halo. Broad peaks for 1-10% NC are seen at 2θ~ 20° as shown in Fig. 6. The disappearance of the characteristic peak at 2θ=6.46° (corresponding to the d_{001} spacing of OC. (Fig. 5) indicates the disordered exfoliated structure that agrees with others [15, 20, 24]. Our XRD results agree with the results of Yeh et al. [4] only at 1% clay loading (CLPS1) where there was a lack of diffraction peak at 2Θ = 2–10°.

However, the rest of formulations at higher clay loading (CLPS5, CLPS10) showed a shift in the characteristic peak for the XRD to lower angels (higher d spacing). On the other hand, other studies found a different trend where the XRD structures did not lose the original diffraction peaks. Examples are Lee et al. [9] who prepared polyaniline/montmorillonite nanocomposites. The reflection peak of the pristine Na^{+}-MMT was at around 2Θ ~9 °. Upon the intercalation of polyaniline, the interlayer spacing is expanded from 9.7-14.3 Å. Thus, the expansion in the interlayer spacing observed was only about 4.6 Å and indicates the insertion of PANI chains between silicate layers.

In addition, the same phenomenon was found by Paul et al. [19] who prepared the Polymer–clay nanocomposites from commercial polystyrene (PS) and laponite clay. In their study, when they used a high clay loading PS-Clay (10%) the XRD chromatogram retained the original structure. However, when laponite clay was modified with CTAB by ion-exchange reaction, its characteristic peak, i.e. from (001) plane has been shifted to lower angles corresponding to an increase in d-spacing from 15·76 nm to 24·58 nm. The d spacing of 15·76 nm to 24·58 nm seemed strange and might be due to a typing error and should be 15·76 Å to 24·58 Å [19]. It has been observed that XRD analysis can lead to false interpretations of the extent of exfoliation [18]. Many factors can influence the XRD patterns of layered silicates such as concentration, or the detection limit of the measuring system [19, 20]. Thus, TEM studies are necessary to fully characterize the nanocomposite.

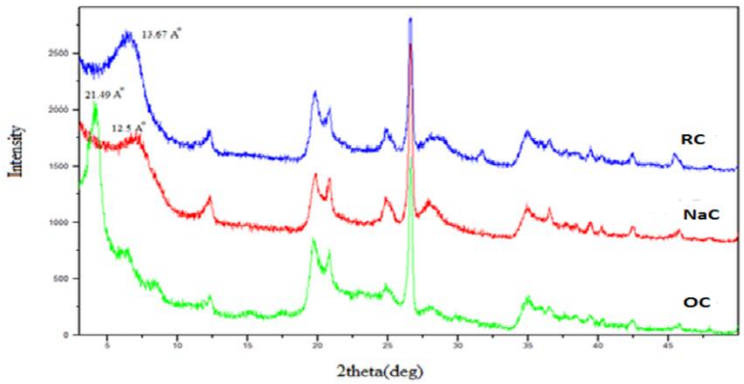

Fig. 5. XRD of RC, NaC and OC.

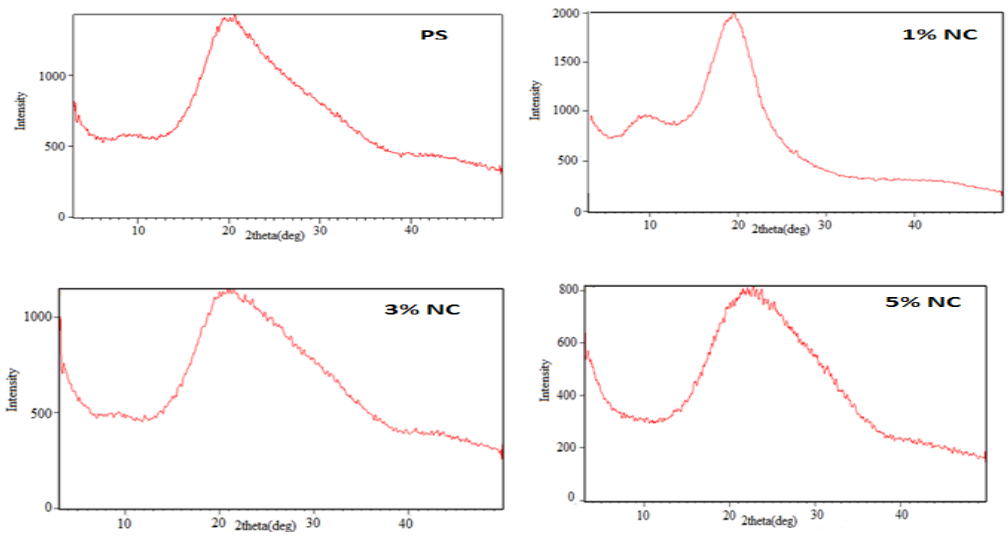

Fig. 6. XRD of PS, OC and 1-10 %NC.

3.4. Transmission Electron Microscope (TEM)

The morphological structures of a series of PS/OC nanocomposites prepared at 1-10 % NC of OC are studied by TEM as shown in Fig. 7. The light regions represent polystyrene matrix and the dark lines are the silicate layers dispersed in the polymer matrix. All of the images show that exfoliated structure was obtained for the low loading (1-5% NC). These morphologies are in excellent agreement with the XRD observations and with other studies [10, 15-17, 24]. However, at high loading there was mixed intercalated-exfoliated structures for 10% NC which is in agreement with other studies as well [4, 9, 12, 18].

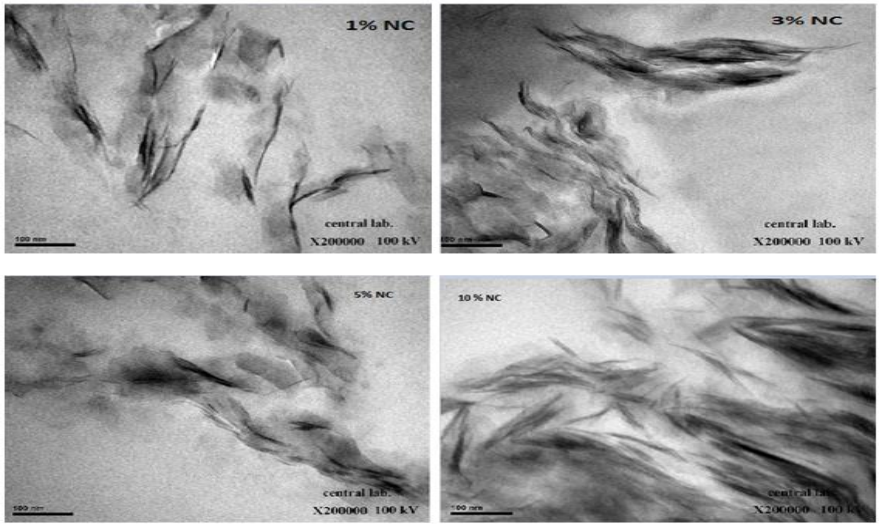

Fig. 7. TEM images of 1%-10 % NC at high magnification.

3.5. Differential Scanning Calorimetry (DSC)

The glass transition temperature, T_g, of a polymer is an important indicator of its thermal properties. DSC analysis of neat polymer and PS/OC nanocomposites are presented in Fig.8. The glass transition temperature decreased from 98.14^{o}C for pure PS to lower values for 1-3% NC then increased slightly for 5% NC to reach a higher T_g of 104.22 ^{o}C at 10% NC. The exfoliated structure that leads to the movement of the polymer chains between the clay layers, so T_g of these PCN (1-5% NC) decreased compared to pure PS. This means that the polymer film became softer with increasing clay loading from 1 to 5 %. So the PS film becomes ductile and does not break when used as a coating material. An increase in T_g for 10% NC indicates limitations to chain segment mobility induced by OC as a results of intercalation of polystyrene chains between OC lamellae. So there is a strong interaction between PS matrix and OC within the silicate sheets that restrict the segmental motion of the polymer chains. The restricted segmental motions within the galleries shift the glass transition temperature to higher values as found by other studies [4, 5, 19, 20].

The values of T_g from the present results are opposite to Yeh et al. results where T_g of PS was 86.5°C, and increased gradually to reach 99.4 ^{o}C at 10% (CLPS10) [4]. Some authors suggest that the decrease in T_g could not be attributed to the organic modifier. If this is the case, all clay nanocomposites should show a lower T_g. Again, this is likely a more general effect of the specific enthalpy interactions. The effect of the nanoparticle on the T_g can be explained by the enthalpic interactions between the polymer and the nanoparticles [4, 20].

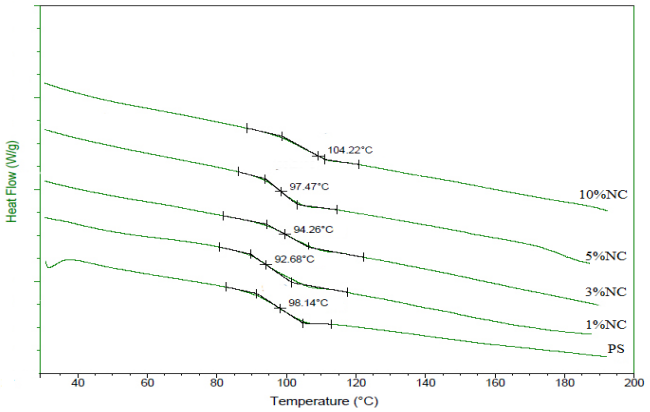

Fig. 8. DSC graph of PS and 1-10% NC.

4. Conclusion

In this investigation, a series of PS-clay nanocomposite materials were prepared by the surface modification of raw clay.

The as-synthesized PCN materials were characterized by FTIR, XRD and TEM. FTIR confirmed the existence of these intercalated organic agents (surfactant) in the inorganic clay samples.

XRD and TEM proved that the exfoliated structure was obtained for the low clay loading while intercalated structure was probably the predominated form in the case of 10% NC.

Based on DSC results, all of the PCN materials showed a lower T_g value compared to pure PS (except 10%). This decrease reflects the plasticization effect of the organic modifier at low content of OC (1-5% NC).

The successful preparation of these PCN may be further used in food packaging, microelectronics, metal coatings and biotechnology. Our work provides a fabrication process which is simple, of low-cost and feasible.

Acknowledgement

The authors extend their appreciation to the Deanship of Scientific Research at King Saud University for funding the work through the research group project No. RGP-VPP-102.
All authors do not have any conflicts of interest to declare.

References

[1] A. Tracton, Editor, Coating Materials and Surface coatings, CRC Press, New York (2006).
[2] D. Zaarei, A. A. Sarabi, F. Sharif, S.M. Kassiriha, J. Coat. Tech. Res. **5**,241(2008).
[3] S. Qutubuddin, X. Fu, Y. Tajuddin, Polym. Bull. **48,** 143(2002).
[4] J. M. Yeh, S.J. Liou, C.G. Lin, Y. P. Chang, Y. H.Yu, C.F. Cheng, J. App. Polym. Sci. **92** ,1970(2004)..
[5] R. A. Vaia, E.P. Giannelis, Macromolecules,**30** ,8000(1997).
[6] S. Ahmad, F. Zafar, E. Sharmin, N. Garg, M. Kashif, Prog. Org. Coat. **73** , 112(2012).
[7] F. Bergaya, B. Theng, G. Lagaley, Elsevier Publisher, Netherland, (2006).
[8] G. Lagaly, Solid State Ionics, **22** ,43(1986).
[9] P. Piromruen, S. Kongparakul, P. Prasassarakich, Prog. Org. Coat. **77**, 691(2014).
[10] M. Heidarian, M.R. Shishesaz, S.M. Kassiriha, M. Nematollahi, Prog. Org. Coat. **68**, 180(2010).

[11] A. Olad, A. Rashidzadeh, Prog. Org. Coat. **62** ,293(2008).
[12] D. Lee, K. Char, S. W. Lee, Y. W. Park, J. Mat. Chem. **13**, 2942(2003).
[13] W.K. Mekhamer, J. Saudi Chem. Soc. **14**, 301(2010).
[14] M. H. Al-Qunaibit, L. A. Al Juhaiman, Inter. J. Basic & App. Sci. **12**, 205 (2012).
[15] J. M. Yeh, C.T. Yao, C.F. Hsieh, L.H. Lin, P.L. Chen, J. C. Wu, H.C. Yang, C.P. Wu, Eur. Polym. J. **44** ,3046 (2008).
[16] S. Yalcinkaya Erdem, N. Yildiz, M. Sac¸ak, A. Calimli, Turk. J. Chem. **34** ,581(2010).
[17] M.Yuehonga, Z. Jianxi, H. Hongpinga, Y. Penga, S. Weia, L. Donga, Spectrochim. Acta A., **77**,122 (2010).
[18] Y. Xi, Z. Ding, R. L. Frost, J. Colloid Interf. Sci. **227** , 116(2004).
[19]P. K. Paul, S. A. Hussain, D. Bhattacharjee, M. Pal, Bull. Mat. Sci. **36** , 361(2013).
[20] A. Giannakas, C. G. Spanos, N. Kourkoumelis, T. Vaimakis, A. Ladavos, Eur. Polym. J. **44** ,3915(2008).
[21] A. Navarchian, M. Joulazadeh, F. Karimi. Prog. Org. Coat. **77** , 347(2014).
[22] J.T. Zhang, J.M. Hu, J.Q. Zhang, C.N. Cao, Prog. Org. Coat. **49** , 293(2004).
[23] K. C .Chang, S. T.Chen, H. F. Lin, C. Y. Lin, H. H. Huang, H. H. Yeh, Y. H. Yu, Euro. Polym. J. **44** ,13(2008)..
[24] X. Fu, S. Qutubuddin, Mater. Lett. **2** ,12(2000).
[25] D. R. Yei, S. W. Kuo, Y. C. Su, F.C. Chang, Polymer, **45** ,2633(2004).
[26] A. Arora, V. Choudhary, D. K. Sharma, J. Polym. Res. **18** ,843(2011).
[27] M. Alshabanat, A. Al-Arrash, W. Mekhamer, J. Nanomater. (2013).Article ID 650725. Retrieved from: http://dx.doi.org/10.1155/2013/650725
[28] A. Kumar, Madhan, Z. M. Gasem, Prog. Org. Coat. **78**,387(2015).